nature photonics

LETTERS

PUBLISHED ONLINE: 20 MAY 2012 | DOI: 10.1038/NPHOTON.2012.110

Avalanche amplification of a single exciton in a semiconductor nanowire

Gabriele Bulgarini[1†]*, Michael E. Reimer[1†], Moïra Hocevar[1], Erik P. A. M. Bakkers[1,2], Leo P. Kouwenhoven[1] and Val Zwiller[1]

Interfacing single photons and electrons is a crucial element in sharing quantum information between remote solid-state qubits[1–8]. Semiconductor nanowires offer the unique possibility of combining optical quantum dots with avalanche photodiodes, thus enabling the conversion of an incoming single photon into a macroscopic current for efficient electrical detection. Currently, millions of excitation events are required to perform electrical readout of an exciton qubit state[1,6]. Here, we demonstrate multiplication of carriers from only a single exciton generated in a quantum dot after tunnelling into a nanowire avalanche photodiode. Owing to the large amplification of both electrons and holes (>10^4), we reduce by four orders of magnitude the number of excitation events required to electrically detect a single exciton generated in a quantum dot. This work represents a significant step towards achieving single-shot electrical readout and offers a new functionality for on-chip quantum information circuits.

Semiconductor quantum dots have been proposed as fundamental elements of a quantum information processor[9]. Quantum bits (qubits) can be stored in the spin state of a single electron[3,4], in the spin state of a single hole[5] or in the bright exciton state[2,8]. Of these, exciton qubits are particularly attractive for achieving long-distance quantum communication by exciton-to-photon and photon-to-exciton transfer of quantum information[10,11]. Coherent optical control of a single exciton qubit in quantum dots has been demonstrated with both optical[8] and electrical[1,6] readout. However, current readout schemes require millions of excitation events to produce a measurable signal. To reduce the number of required excitation events (with the ultimate aim of single-shot measurements), an internal pre-amplification of the electrical signal is desirable. Avalanche photodiodes (APD) provide this high internal gain and generate a macroscopic current in response to a single absorbed photon[12]. As a result, single photons can be detected efficiently[13]. The avalanche process has been shown at the nanoscale using semiconductor nanowires[14–16] and carbon nanotubes[17], with sensitivity limited to, at best, ~100 photons. Importantly, semiconductor nanowires grown using bottom-up techniques offer an unprecedented material freedom in growing advanced heterostructures[18,19] due to the reduced strain achieved in the growth of highly mismatched materials[20]. Potentially, heterostructured[21] and electrically defined[7] quantum dots can be combined within the same nanowire for quantum information processing.

In this Letter, we demonstrate the integration of a single quantum dot in the avalanche multiplication region of a nanowire photodiode in a configuration that demonstrates high internal gain and sensitivity to single photons. By spectrally and spatially separating the absorption region from the multiplication region, we can selectively generate a single exciton in the quantum dot that is efficiently multiplied after tunnelling in the nanowire depletion region under an applied electric field. We characterize the nanowire internal gain by photocurrent measurements down to the single photon regime. Finally, we show that only 120 individual excitation events are required to perform electrical readout of an exciton confined in a single quantum dot.

A scanning electron microscopy (SEM) image of our device containing a single quantum dot embedded in a contacted InP nanowire is presented in Fig. 1a. The InP nanowire was doped *in situ* during vapour–liquid–solid growth to obtain a p–n junction (see Methods). The depletion region of the p–n junction was used to multiply both electrons and holes as they gain enough energy to initiate the avalanche multiplication process. The operating principle of our nanowire APD is shown schematically in Fig. 1b,c. A single photon incident on the device with a frequency equal to one of the quantum dot transitions is absorbed and creates a single exciton. Under reverse bias ($V_{sd} < 0$), the electron and hole separate and tunnel into the nanowire depletion region. Both the electron and hole then accelerate under the applied electric field and, once the carriers gain enough energy, additional electron–hole pairs are created by impact ionization. These additional electron–hole pairs can further trigger carrier multiplication and strongly enhance the photocurrent. The final result is that each exciton created in the quantum dot is multiplied into a macroscopic current. A unique feature of InP nanowires is that the impact ionization energy is similar for both electrons and holes (1.84 eV and 1.65 eV, respectively)[22]. Both carriers can thus contribute to the avalanche multiplication process and large gains can be achieved.

In Fig. 1d we probe the quantum dot and nanowire absorption spectra by tuning the laser excitation wavelength. The measured photocurrent shows a broad absorption peak around 825 nm originating from InP band-edge transitions, which suggests the presence of both wurtzite and zincblende crystal structures, as confirmed by transmission electron microscopy (TEM)[23]. Three equally spaced photocurrent peaks are observed at higher excitation wavelengths (1,007, 986 and 963 nm). By comparing these with typical photoluminescence spectroscopy of single quantum dots in intrinsic nanowires (Supplementary Fig. S1), we assign these three peaks to absorption in the quantum dot *s*, *p* and *d* shells, respectively. From photoluminescence spectroscopy of the device at $V_{sd} = 0$ V, we confirm that the peak at 1,007 nm is due to absorption in the quantum dot ground state (*s*-shell). The observed shell separation of 26 meV corresponds to a diameter of ~27 nm according to calculations that assume an in-plane parabolic confinement in the quantum dot and is in agreement with the quantum dot size measured with TEM[24].

We now characterize the photoresponse of the nanowire APD. Optical excitation above both InP and InAsP bandgaps was used

[1]Kavli Institute of Nanoscience, Delft University of Technology, 2628 CJ Delft, The Netherlands, [2]Eindhoven University of Technology, 5600 MB Eindhoven, The Netherlands; [†]These authors contributed equally to this work. *e-mail: g.bulgarini@tudelft.nl

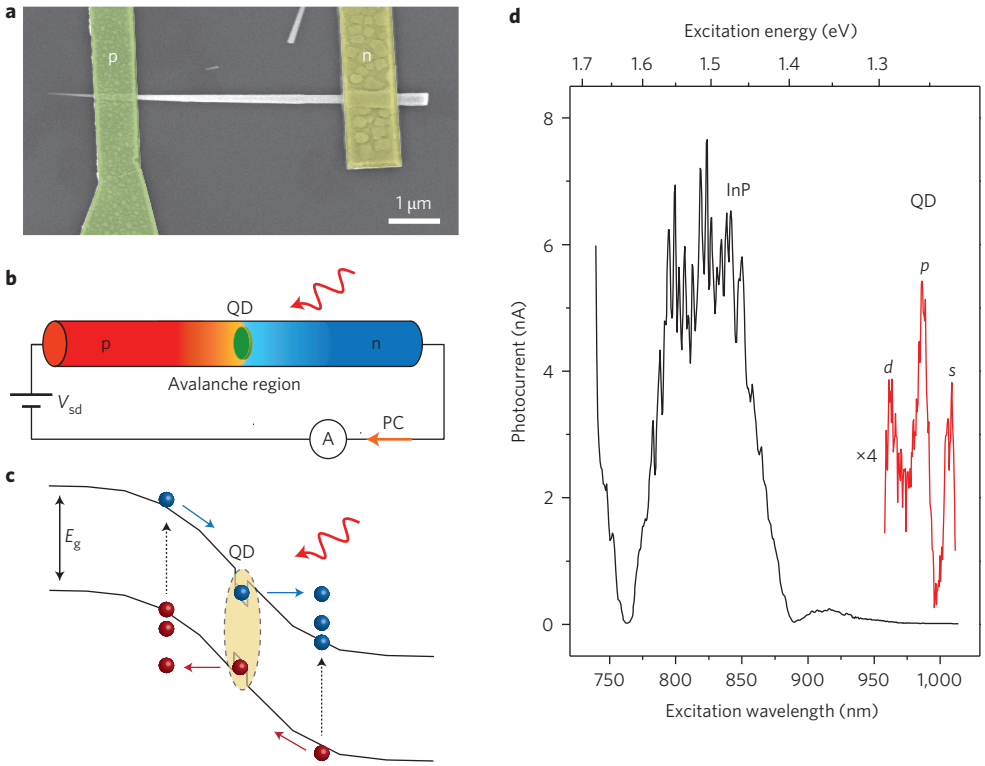

Figure 1 | Single quantum dot in a nanowire APD. a, SEM image of the nanowire photodiode. **b**, A single quantum dot (QD) is located within the nanowire depletion region, where avalanche multiplication of the photocurrent (PC) is achieved under reverse voltage bias, V_{sd}. **c**, Schematics of carrier multiplication starting from an exciton generated in the quantum dot, followed by tunnelling in the nanowire avalanche region. **d**, Photocurrent spectroscopy at $V_{sd} = -2$ V with 1 μW and 20 μW excitation powers (black and red curves, respectively). Band-edge absorption in the nanowire is observed around 825 nm (black). Absorption in the quantum dot *s*, *p* and *d* shells is observed at longer wavelengths (red).

to excite the entire nanowire depletion region and measure the resulting multiplication gain. We used a 120 Hz mechanically chopped continuous-wave laser at a wavelength of $\lambda = 532$ nm, which was linearly polarized along the nanowire elongation axis to maximize absorption. The inset of Fig. 2a shows the temporal response of the photocurrent (blue line) to the laser trigger (dashed black line). We obtained a time constant of 1 ms, which is a direct result of the high resistance of the device (60 MΩ). Current–voltage characterization of the device is shown in the main panel of Fig. 2a as a function of incident optical power on the sample. At $V_{sd} = 0$ V, only the p–n junction built-in electric field separates electron–hole pairs to produce a measurable photocurrent without multiplication gain. Here, we measured a linear dependence for the ratio of charge carriers collected at the contacts to the number of photons absorbed by the nanowire, which was obtained by estimation of the absorption efficiency (~0.3%, see Methods). We determine that a single photon absorbed in the nanowire is converted into one electron (hole) worth of current with 96% probability (Supplementary Fig. S2). This efficiency is comparable to state-of-the-art nanowire solar cells[25] and conventional quantum dot photodiodes[1]. In the reverse bias region ($V_{sd} < 0$), the dark current is less than 1 pA until an avalanche breakdown occurs at $V_{sd} = -15$ V, as shown in Supplementary Fig. S3. Under illumination, the photocurrent increases rapidly for applied reverse bias larger than $V_{sd} \approx -1$ V, because the absorption of a photon triggers an avalanche multiplication of carriers. The multiplication gain reaches saturation at stronger applied electric fields and, at saturation, the photodiode current–voltage slope is set by the total series resistance, which decreases at higher photon flux. The occurrence of a light-induced avalanche at rather low applied bias is due to the use of a small depletion region (~200 nm) and the low impact ionization energy threshold of InP. This photoresponse is reproducible, and similar behaviour was observed in six different devices.

In Fig. 2b, the excitation pulses are strongly attenuated to investigate the multiplication gain in the few-photon regime. The device was operated below breakdown voltage at saturation of the light-induced avalanche multiplication ($V_{sd} = -8$ V) and at a temperature of 40 K to optimize the signal-to-noise ratio of the photocurrent (Supplementary Fig. S4). Each experimental data point (black circles) corresponds to the current averaged over 120 excitation pulses and with the dark current subtracted to obtain the net photocurrent. From the linear fit (blue line) to the experimental data, we determine an internal gain of $G_i = 2.3 \times 10^4$. This high multiplication factor, combined with the low noise of the device (~0.2 pA), enables the detection of a single photon absorbed per excitation pulse. The measured gain is in very good agreement with calculations reported in the Supplementary Information, Page 10 that assume both carriers contribute to the avalanche multiplication process. The sensitivity to single photons is confirmed by measuring the photocurrent after individual excitation pulses. In Fig. 2c, the current measured with, on average, one photon per pulse (red circles) is compared to the dark current (black crosses). The absorption of a single photon yields a signal that can be distinguished readily from the dark current, with a signal-to-noise ratio of 2.5. The detection of single photons from an individual InP nanowire does not therefore require averaging over multiple excitation events or the use of lock-in amplification. The estimation of the number of photons absorbed per excitation pulse was confirmed by photon counting measurements (Supplementary Fig. S5) in the few-photon regime, which are described well by Poisson statistics.

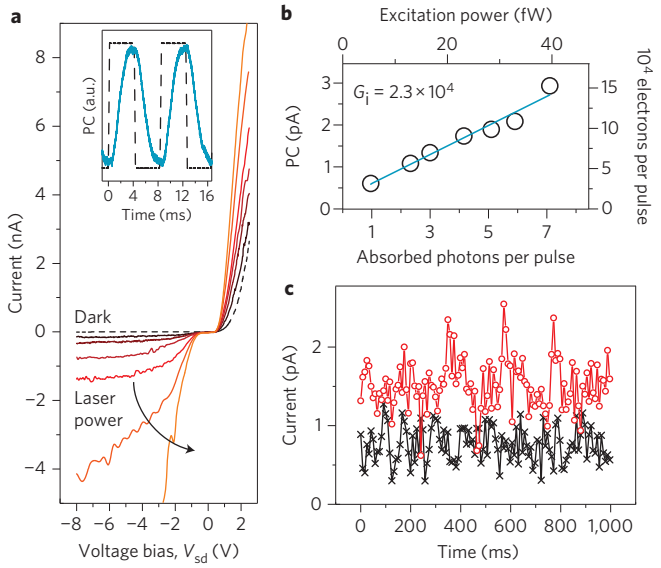

Figure 2 | Single photon detection with a nanowire photodiode. a, Main panel: electrical characteristics of the device in the absence of illumination (dashed line) and as a function of incident optical power (100 pW, black; 100 nW, orange) at $\lambda = 532$ nm (coloured curves). Inset: photocurrent temporal response (blue line) to 120 Hz laser pulses (black dashed line). **b**, Nanowire photodiode response in avalanche operation at $V_{sd} = -8$ V. Photocurrent (PC) is obtained by subtracting the dark current from the current measured with illumination. The high multiplication gain of 2.3×10^4 and low noise (0.2 pA) enables the detection of one absorbed photon per excitation pulse **c**, Absorption of one photon per pulse yields a signal (red circles) that is well distinguished from the dark current (black crosses).

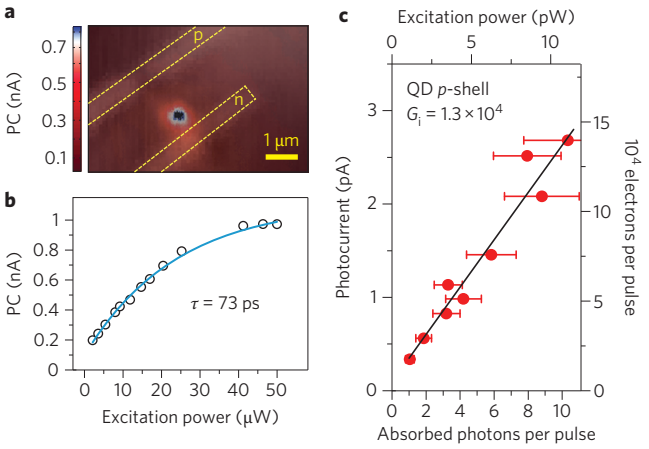

Figure 3 | Resonant single photon detection in the quantum dot. **a**, A photocurrent (PC) image for quantum dot *p*-shell excitation is superimposed on a laser reflection image. As expected, the maximum occurs within the p–n junction where the quantum dot is located. **b**, Quantum dot *p*-shell photocurrent under continuous-wave excitation at zero applied bias. From the exponential fit (blue line) we determine the tunnelling time τ of 73 ps for the slowest of the two carriers. **c**, At $V_{sd} = -8$ V, we obtain a gain of 1.3×10^4 for each photon generated in the quantum dot *p*-shell. Error bars (~30%) represent the variance in the measured quantum dot height.

In the following, we use the single quantum dot as the only absorption region of the nanowire photodiode. We selectively excite only the quantum dot *p*-shell transition and use the nanowire as an efficient multiplication channel for the photogenerated exciton. In Fig. 3a we measure the photocurrent from the *p*-shell resonance as a function of laser spot position. The photocurrent image is superimposed with a laser reflection image to exclude contribution from Schottky contacts. The photocurrent maximum is reached when the laser spot impinges between the metallic contacts. The same photocurrent maximum position is obtained when exciting the entire nanowire at $\lambda = 532$ nm, confirming that, as expected, the quantum dot is positioned within the nanowire depletion region.

In Fig. 3b, we resonantly pump the quantum dot *p*-shell with continuous-wave excitation at zero applied bias, corresponding to a built-in electric field of 70 kV cm^{-1}. We observe a saturation of the photocurrent at $I_{sat} \approx 1$ nA for high excitation power, as the current is limited by the tunnelling time τ of the generated electron and hole. From the exponential fit to the data, we determine the tunnelling time of the slowest carrier, $\tau = e/2I_{sat} = 73$ ps, similarly to ref. 26. The tunnelling time represents the ultimate limit to the coherence of the exciton qubit. We note that the tunnelling time can be extended by reducing the electric field strength[26], for example, by surrounding the quantum dot with an intrinsic region.

Finally, we estimate the gain obtained after a single photon is resonantly absorbed in the quantum dot *p*-shell and tunnels into the nanowire multiplication region at $V_{sd} = -8$ V. Remarkably, we measure a large multiplication gain of 1.3×10^4 (Fig. 3c). As a result, the generation of a single exciton in the quantum dot is detected using a low excitation rate of 120 Hz, where only a single photon is absorbed in the quantum dot per excitation pulse. The number of charge carriers collected per absorbed photon is four orders of magnitude larger than previously reported for self-assembled quantum dots embedded in diode structures[1], and seven orders of magnitude larger than for photodetectors based on a single contacted quantum dot in a nanowire[27].

We have demonstrated that InP nanowires provide an efficient one-dimensional channel for electrical transport, where electrons and holes undergo impact ionization with high probability, thereby achieving large multiplication factors. The significant gain ($>10^4$) we report for resonant absorption in a single quantum dot is promising in the drive towards achieving single-shot electrical readout of an exciton qubit state for the transfer of quantum information between flying and stationary qubits[10,11]. The extremely small active area represents the fundamental limit to the device external efficiency, which can be enhanced by light harvesting with plasmonic antennas[28] and by reducing the optical excitation spot size with a solid immersion lens[29]. On the other hand, in the present configuration the quantum dot absorption region is spectrally and spatially separated from the multiplication region. The material freedom available during nanowire growth enables engineering of the quantum dot absorption properties, while conserving single photon sensitivity with a unique subwavelength spatial resolution.

Methods

Device fabrication. InP nanowire p–n junctions containing InAsP quantum dots were grown using a vapour–liquid–solid mechanism with gold catalysts (diameter, 20 nm). Growth was performed in a metal–organic vapour phase epitaxy (MOVPE) reactor at a pressure of 50 mbar. Tri-methyl-indium and phosphine were used as precursors for nanowire growth and arsine was added during quantum dot growth. n-Doping was achieved with hydrogen sulphide, and diethyl-zinc was used for p-doping. Growth was initiated with the n-InP section, followed by the InAsP quantum dot and the p-InP section. The quantum dot height was 6 ± 2 nm and the diameter ~30 nm. Subsequent to growth, the nanowires were transferred onto a SiO_2/silicon substrate and contacts were defined by electron-beam lithography. The n-sides of the nanowires were contacted with evaporated titanium/gold (100/10 nm), and titanium/zinc/gold (1.5/30/70 nm) was used for the p-contacts. Because the p-contact demonstrates Schottky behaviour, rapid thermal annealing at 350 °C was performed to induce zinc diffusion from the contact into the nanowire, thus reducing the Schottky barrier width. After annealing, the typical device series resistance was decreased by three orders of magnitude (to a few tens of MΩ) to reduce the photodiode response time. We expect the RC constant to be

reduced in future work by decreasing the separation between the two contacts and improving the contact resistance to the nanowire. However, in contrast to conventional quantum dot photodiodes[1,6,26], the ultimate limit to the response time of an APD is set by the recovery time of the avalanche process.

Photon number estimation. To estimate the number of absorbed photons per pulse, we first calculated the overlap of the nanowire active area with the laser spot, assuming a rectangular nanowire cross-section. The overall absorption efficiency η_{abs} was then determined using the calculated overlap and bulk InP absorption coefficients[30], taking into account reflections at the nanowire–air and nanowire–SiO_2 interfaces. Finally, the number of photons in a laser pulse was measured with a calibrated power meter to obtain the number of absorbed photons, $P/(h\nu) \times \eta_{abs}$, where P is the laser power and $h\nu$ is the energy of a single photon. Laser transmission through the filters and optical elements forming the optical excitation path was measured to calibrate the optical power impinging on the sample. Photon counting measurements performed in the few-photon regime confirmed estimations of the absorbed photon rates. For details, see Supplementary Fig. S5.

The laser spot size was measured by photocurrent imaging and was determined to be 1.2 μm for $\lambda = 532$ nm and 1.8 μm for $\lambda = 986$ nm (quantum dot p-shell). The photodiode active area was determined by SEM imaging and by four-point resistivity measurements (Supplementary Fig. S6) to obtain doping concentrations for the p–n junction. Resistivity measurements were performed on homogeneous n- and p-doped InP nanowires, which had been grown under the same conditions as the nanowire p–n junction. From the measured doping levels of 1×10^{18} cm^{-3} for the n-side and 1×10^{17} cm^{-3} for the p-side, we estimate a p–n junction depletion region width of 140 nm at $V_{sd} = 0$ V.

The calculated absorption efficiency for $\lambda = 532$ nm at $V_{sd} = 0$ V is 0.3%. The active area of the photodiode (that is, the depletion region) increases with applied reverse bias (370 nm at –8 V), resulting in a higher absorption efficiency of 0.8%. The estimate for the absorption efficiency is only valid for polarization aligned along the nanowire axis, as the absorption for polarization perpendicular to the nanowire is strongly suppressed (Supplementary Fig. S7). The absorption efficiency obtained under resonant excitation in the quantum dot is 0.003%. The main source of error for the absorption efficiency is related to measurement of the height of the quantum dot. We took this error into account with the error bars (~30%) in Fig. 3c.

Received 19 December 2011; accepted 12 April 2012; published online 20 May 2012

References

1. Zrenner, A. *et al.* Coherent properties of a two-level system based on a quantum-dot photodiode. *Nature* **418,** 612–614 (2002).
2. Li, X. *et al.* An all-optical quantum gate in a semiconductor quantum dot. *Science* **301,** 809–811 (2003).
3. Koppens, F. H. L. *et al.* Driven coherent oscillations of a single electron spin in a quantum dot. *Nature* **442,** 766–771 (2006).
4. Press, D., Ladd, T. D., Zhang, B. & Yamamoto, Y. Complete quantum control of a single quantum dot spin using ultrafast optical pulses. *Nature* **456,** 218–221 (2008).
5. Brunner, D. *et al.* A coherent single-hole spin in a semiconductor. *Science* **325,** 70–72 (2009).
6. Michaelis de Vasconcellos, S., Gordon, S., Bichler, M., Meier, T. & Zrenner, A. Coherent control of a single exciton qubit by optoelectronic manipulation. *Nature Photon.* **4,** 545–548 (2010).
7. Nadj-Perge, S., Frolov, S. M., Bakkers, E. P. A. M. & Kouwenhoven, L. P. Spin–orbit qubit in a semiconductor nanowire. *Nature* **468,** 1084–1087 (2010).
8. Benny, Y. *et al.* Coherent optical writing and reading of the exciton spin state in single quantum dots. *Phys. Rev. Lett.* **106,** 040504 (2011).
9. Loss, D. & DiVincenzo, D. P. Quantum computation with quantum dots. *Phys. Rev. A* **57,** 120–126 (1998).
10. Vrijen, R. & Yablonovitch, E. A spin-coherent semiconductor photo-detector for quantum communication. *Physica E* **10,** 569–575 (2001).
11. Kosaka, H. *et al.* Spin state tomography of optically injected electrons in a semiconductor. *Nature* **457,** 702–705 (2009).
12. Capasso, F. Band-gap engineering: from physics and materials to new semiconductor devices. *Science* **235,** 172–176 (1987).
13. Kardynal, B. E., Yuan, Z. L. & Shields, A. J. An avalanche-photodiode-based photon-number-resolving detector. *Nature Photon.* **2,** 425–428 (2008).
14. Yang, C., Barrelet, C. J., Capasso, F. & Lieber, C. M. Single p-type/intrinsic/n-type silicon nanowires as nanoscale avalanche photodetectors. *Nano Lett.* **6,** 2929–2934 (2006).
15. Hayden, O., Agarwal, R. & Lieber, C. M. Nanoscale avalanche photodiodes for highly sensitive and spatially resolved photon detection. *Nature Mater.* **5,** 352–356 (2006).
16. Reimer, M. E. *et al.* Single photon emission and detection at the nanoscale utilizing semiconductor nanowires. *J. Nanophoton.* **5,** 053502 (2011).
17. Gabor, N. M., Zhong, Z., Bosnick, K., Park, J. & McEuen, P. L. Extremely efficient multiple electron–hole pair generation in carbon nanotube photodiodes. *Science* **325,** 1367–1371 (2009).
18. Tomioka, K., Motohisa, J., Hara, S., Hiruma, K. & Fukui, T. GaAs/AlGaAs core multishell nanowire-based light-emitting diodes on Si. *Nano Lett.* **10,** 1639–1644 (2010).
19. Heurlin, M. *et al.* Axial InP nanowire tandem junction grown on a silicon substrate. *Nano Lett.* **11,** 2028–2031 (2011).
20. Messing, M. E. *et al.* Growth of straight InAs-on-GaAs nanowire heterostructures. *Nano Lett.* **11,** 3899–3905 (2011).
21. Minot, E. D. *et al.* Single quantum dot nanowire LEDs. *Nano Lett.* **7,** 367–371 (2007).
22. Pearsall, T. P. Threshold energies for impact ionization by electrons and holes in InP. *Appl. Phys. Lett.* **35,** 168–170 (1979).
23. Algra, R. E. *et al.* Twinning superlattices in indium phosphide nanowires. *Nature* **456,** 369–372 (2008).
24. Reimer, M. E. *et al.* Bright single-photon sources in bottom-up tailored nanowires. *Nature Commun.* **3,** 737 (2012).
25. Kelzenberg, M. D. *et al.* Enhanced absorption and carrier collection in Si wire arrays for photovoltaic applications. *Nature Mater.* **9,** 239–244 (2010).
26. Beham, E., Zrenner, A., Findeis, F., Bichler, M. & Abstreiter, G. Nonlinear ground-state absorption observed in a single quantum dot. *Appl. Phys. Lett.* **79,** 2808–2810 (2001).
27. van Kouwen, M. P. *et al.* Single quantum dot nanowire photodetectors. *Appl. Phys. Lett.* **97,** 113108 (2010).
28. Curto, A. G. *et al.* Unidirectional emission of a quantum dot coupled to a nanoantenna. *Science* **329,** 930–933 (2010).
29. Stotz, J. A. H. & Freeman M. R. A stroboscopic scanning solid immersion lens microscope. *Rev. Sci. Instrum.* **68,** 4468–4477 (1997).
30. Aspnes, D. E. & Studna, A. A. Dielectric functions and optical parameters of Si, Ge, GaP, GaAs, GaSb, InP, InAs, and InSb from 1.5 to 6.0 eV. *Phys. Rev. B* **27,** 985–1009 (1983).

Acknowledgements

The authors thank J. Rarity and S.M. Frolov for useful scientific discussions. This work was supported by the Netherlands Organization for Scientific Research (NWO), the Dutch Organization for Fundamental Research on Matter (FOM), the European Research Council and a DARPA QUEST grant.

Author contributions

The experiments were conceived and designed by G.B., M.E.R. and V.Z., and were carried out by G.B. and M.E.R. The sample was grown by M.H. and E.P.A.M.B. and contacted by M.E.R. The data were analysed by G.B., M.E.R. and V.Z. The manuscript was written by G.B. and M.E.R. with input from M.H., E.P.A.M.B., L.P.K. and V.Z.

Additional information

The authors declare no competing financial interests. Supplementary information accompanies this paper at www.nature.com/naturephotonics. Reprints and permission information is available online at http://www.nature.com/reprints. Correspondence and requests for materials should be addressed to G.B.